

# Cytotoxicity Study of Ionophore-Based Membranes: Toward On-Body and in Vivo Ion Sensing

Rocío Cánovas,<sup>†</sup> Sara Padrell Sánchez,<sup>‡</sup> Marc Parrilla,<sup>†</sup> María Cuartero,<sup>†</sup> and Gastón A. Crespo<sup>\*,†</sup>

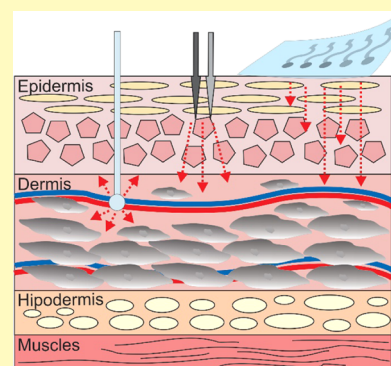
<sup>†</sup>Department of Chemistry, School of Engineering Science in Chemistry, Biotechnology and Health, KTH Royal Institute of Technology, Teknikringen 30, SE-100 44 Stockholm, Sweden

<sup>‡</sup>Department of Clinical Science, Intervention and Technology, Karolinska Institutet, and Division of Obstetrics and Gynecology, Karolinska Universitetssjukhuset, SE-141 86 Stockholm, Sweden

## Supporting Information

**ABSTRACT:** We present the most complete study to date comprising in vitro cytotoxicity tests of ion-selective membranes (ISMs) in terms of cell viability, proliferation, and adhesion assays with human dermal fibroblasts. ISMs were prepared with different types of plasticizers and ionophores to be tested in combination with assays that focus on the medium-term and long-term leaching of compounds. Furthermore, the ISMs were prepared in different configurations considering (i) inner-filling solution-type electrodes, (ii) all-solid-state electrodes based on a conventional drop-cast of the membrane, (iii) peeling after the preparation of a wearable sensor, and (iv) detachment from a microneedle-based sensor, thus covering a wide range of membrane shapes. One of the aims of this study, other than the demonstration of the biocompatibility of various ISMs and materials tested herein, is to create an awareness in the scientific community surrounding the need to perform biocompatibility assays during the very first steps of any sensor development with an intended biomedical application. This will foster meeting the requirements for subsequent on-body application of the sensor and avoiding further problems during massive validations toward the final in vivo use and commercialization of such devices.

**KEYWORDS:** biocompatibility, cytotoxicity tests, ion-selective electrodes, biomedical applications, point-of-care



In view of the increasing demand for wearable sensors and point-of-care tools, claiming to reformulate the current health-care system,<sup>1–3</sup> it is worthwhile establishing effective protocols to critically assess biocompatibility features of materials used in the fabrication of these devices. In this regard, biocompatibility is a term frequently used to describe the functionality of materials in contact with biological samples, and according to the IUPAC, it refers to the “ability of any material to be in contact with a living system without producing an adverse effect”.<sup>4</sup>

Assays based on cytotoxicity<sup>5</sup> (tissue culture), sensitization, irritation and inflammatory tests,<sup>6</sup> genotoxicity,<sup>7,8</sup> hemocompatibility,<sup>9</sup> and carcinogenesis,<sup>8</sup> among others, are often utilized to evaluate the biocompatibility of sensing devices with biomedical purposes. More specifically, cytotoxicity evaluates either the toxic effect of a material or chemical compound in mammalian cell cultures after a certain exposure period<sup>6</sup> and has been so far assessed through in vitro assays.<sup>10</sup> Indeed, this latter technique is very valuable for providing essential information as a preliminary screening of the potential toxicity or viability of a material when using any of its variants: the study of cell growth, adhesion, proliferation, and/or morphological effects.<sup>5</sup> In addition, classical in vitro cytotoxicity assays possess advantages of simplicity, cost-effectiveness, swiftness, few ethical issues, as well as the minimization of

animal trails in the initial stage of the development of a medical device.<sup>11</sup>

Importantly, from the very beginning conception of the sensor to be used in a specific biomedical application, it is necessary to assure the biocompatibility of each material used for its fabrication, as well as the engineered device. However, biocompatibility requirements strongly vary in relation to the way that the device interacts with the human body as the direct contact of the sensor with any part of the individual’s body, exposure time, and possible alteration/degradation of the materials involved may lead to a change in its toxicity. For example, as illustrated in Figure 1, sensors may be worn on the body (i.e., a wearable sensor attached to the skin),<sup>12–14</sup> partially embedded into the body (i.e., the sensor penetrates the first body barrier but without reaching the dermis, as in the case of microneedle-based sensors),<sup>15–19</sup> or implanted in the body (i.e., a sensor that reaches the bloodstream or interact with organs).<sup>20–23</sup>

Despite the significance of evaluating any toxic effects coming from the leaching of chemicals and/or materials from the sensing device, no matter the configuration, it is also true that as long as invasiveness becomes more pronounced, other

Received: July 15, 2019

Accepted: August 26, 2019

Published: August 26, 2019

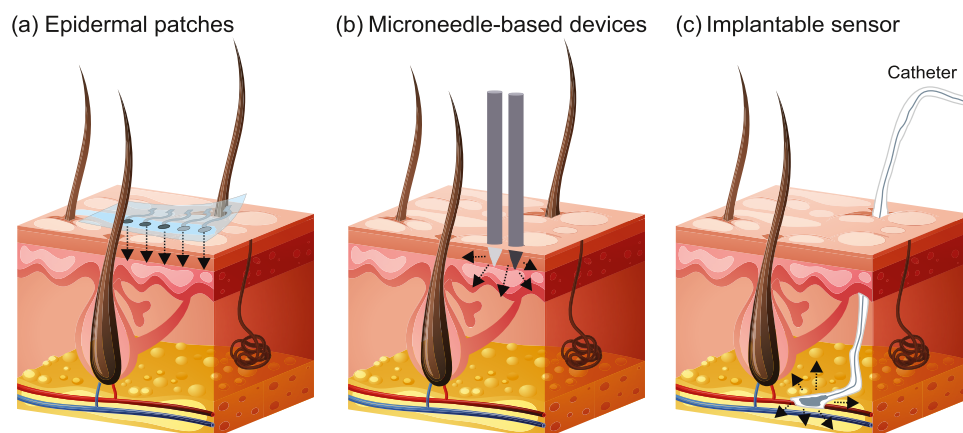


**Figure 1.** Illustration of the different configurations of sensors for on-body measurements: (a) wearable sensor based on traditional epidermal patch; (b) microneedle-based sensor penetrating the first body barrier; and (c) implantable sensors. The arrows symbolize the possible leaching of compounds from the sensor.

effects have to be additionally considered. This is the case of the adsorption of proteins on the sensor surface, which may lead to nonspecific biological responses of the body, such as cell adhesion and/or coagulation, presenting potential adverse effects to the individual.<sup>24–27</sup>

Among the types of sensors that can be conceived as point-of-care tools, ion-selective electrodes (ISEs) have attracted increasing attention over the past years owing to simplicity, versatility, rapid responsiveness, cost-effectiveness, miniaturization, and user-friendly nature.<sup>28–30</sup> ISEs are able to monitor minor fluctuations in ion concentrations (strictly speaking, fluctuations in ion activity) related to ongoing processes in diverse samples, such as biological fluids and environmental water among others.<sup>31,32</sup> Accordingly, changes found in ion concentration may be indicative of significant processes occurred in the traced event, of which their interpretation offers valuable information in terms of body status, illness diagnosis, contamination, and so on.<sup>33–36</sup> This information becomes exceptionally relevant when it is attained *in situ* and in real time, as is the case with point-of-care devices.

The most widely employed sensing element of ISEs comprises ion-selective membranes (ISMs), which combine different materials conferring physical robustness (polymer and plasticizer), ion-exchange abilities (ion exchanger), and selectivity toward one specific ion target (receptors, also called ionophores in the sensing parlance).<sup>37–40</sup> Once the development of ISEs at the laboratory scale is foreseen for a biomedical application,<sup>41</sup> the next logical step is to evaluate the biocompatibility of all of the components, particularly those implemented in the ISM, as follows: (i) compatibility of the sensor along with the biological fluid where the analysis is to be accomplished; (ii) adverse reactions of the skin or any other body tissues that is prone to be in contact with the sensor during penetration, insertion, or analytical measurements; and (iii) toxicity as a result of potential leaching of any of the components present in the sensor. These cases are aligned with the possible configurations that the electrode may adopt for on-body measurements (see Figure 1). Furthermore, the compounds comprised in ISMs are also extensively used to prepare reversible optical sensors and, therefore, biocompatibility studies would be also relevant for optical sensors, as well.

To this end, there have been several studies related to the individual toxicity of materials used in the preparation of ISEs, ionophores,<sup>42–44</sup> plasticizers,<sup>40,45,46</sup> ionic liquids,<sup>28</sup> nano-

particles (NPs),<sup>7,47</sup> and carbon nanotubes (CNTs)<sup>9</sup> among others,<sup>48,49</sup> that claim them to be “toxic elements”. Nevertheless, we have identified a lack of cytocompatibility tests involving ISEs, especially those featuring common tissue cells of the skin (i.e., fibroblasts). This is indeed a critical issue as many wearable and implantable ISEs are placed in contact with the skin or nearby deeper human tissues.<sup>50</sup> Therefore, fibroblast-based *in vitro* cytotoxicity assays are crucial because these cells are the most common cell line found in the skin and one of the first barriers to the subcutaneous tissue where blood vessels are located.<sup>51</sup>

Very few publications focused on *in vitro* cytotoxicity assays of ISEs and ISMs are available in the literature up to now. On one hand, Jiang and co-workers recently studied the improved hemocompatibility of calcium-selective electrodes modified with a polydopamine coating through a blood platelet adhesion experiment, which are based on incubation in platelet-rich plasma for 2 h.<sup>25</sup> On the other hand, Meyerhoff et al. used *in vitro* platelet adhesion studies to compare the thrombogenic properties of implantable ISEs based on poly(vinyl chloride) (PVC) and polyurethane (PU) as polymers in ISMs by means of scanning electron microscopy measurements.<sup>26</sup> Both investigations were carried out to improve the biocompatibility of implantable ISEs and both utilized blood platelet adhesion for the cytotoxicity test. To determine the toxicity of these materials, a wider range of cytotoxicity testing would be beneficial in future approaches. Another feature to highlight regarding the aforementioned articles relies on the importance of testing the biocompatibility of wearable ISEs with other cell lines, one of the main concerns of the present work.

The so-called potassium ionophore I (valinomycin) used in ISMs has been evaluated in several works. Daniele and co-workers were the very first to demonstrate the adverse effects of valinomycin as it inhibited phytohemagglutinin-stimulated blastogenesis and proliferation in human lymphocytes.<sup>52</sup> It seems that this inhibition was not the result of pure cell toxicity, but valinomycin exhibited potential action as an uncoupler of oxidative phosphorylation, thereby affecting the proliferation of the cells.<sup>42,52</sup> In addition, other effects, like neurotoxicity,<sup>44</sup> collapsing of the mitochondrial membrane potential,<sup>52,53</sup> apoptosis in certain mammalian cell lines, and sperm mobility inhibition<sup>54</sup> among others, have also been reported. More recently, our group showed the toxic effects of valinomycin with cell viability and proliferation assays on

Table 1. Composition of the Membranes Used in the Cytotoxicity Assays<sup>a</sup>

membrane	I-Ex	ionophores					polymer		plasticizers		solvent
	NaTFPB	K <sup>+</sup>	H <sup>+</sup>	Ca <sup>2+</sup>	Na <sup>+</sup>	NH <sub>4</sub> <sup>+</sup>	PU	DOS	<i>o</i> -NPOE	FNDPE	THF
I (PU + DOS)	0.3						16.5	33			0.5
II (PU + DOS) <sup>b</sup>	0.3						16	33			0.5
III (PU + NPOE)	0.3						16.5		33		0.5
IV (PU + FNDPE)	0.3						16.5			33	0.5
V (KSM) <sup>c</sup>	0.8	2					33	65			1
VI (NH <sub>4</sub> SM)	0.3					0.5	16.5	33			0.5
VII (CaSM)	0.43			0.5			16.5	33			0.5
VIII (NaSM)	0.49				0.7		33	66			1
IX (HSM)	0.38		0.5				16.5	33			0.5
X (KSM) <sup>d</sup>	0.5	1					31.7	67			1
XI (KSM) <sup>c</sup>	1.6	4					66	130			2
XII (KSM) <sup>c</sup>	0.4	1					16.5		32.5		0.5
XIII (KSM) <sup>c</sup>	0.4	1					16.5			32.5	0.5
XIV (PU)							16.5				0.5
XV (PU + NaR)	1						16.5				0.5
XVI (PU + DOS)	0.3						25	25			0.5
XVII (PU + DOS)	0.3						33	16.5			0.5

<sup>a</sup>All of the amounts are expressed in mg less for the solvent, which is expressed in mL. <sup>b</sup>A concentration of 0.5 mg mL<sup>-1</sup> of MWCNTs was added in this membrane composition. <sup>c</sup>Valinomycin as potassium ionophore. <sup>d</sup>Potassium ionophore II. PU = polyurethane; DOS = dioctyl sebacate; NPOE = 2-nitrophenyl octyl ether; FNDPE = 2-fluorophenyl 2-nitrophenyl ether; K = potassium; NH<sub>4</sub> = ammonium; Ca = calcium; Na = sodium; H = hydrogen; NaR = ion exchanger; SM = selective membrane.

fibroblasts as a consequence of leaching from ISMs after 48 h of contact with cell culture.<sup>19</sup> Conversely, in that work, we demonstrated the absence of toxicity of the membrane materials (different plasticizer, ion exchanger, and nanotubes) when they were individually incorporated into either PVC or PU matrix.<sup>19</sup>

Herein, the most complete study to date is presented, as far as we know, comprising in vitro cytotoxicity assessment of ISMs in terms of cell viability, proliferation, and adhesion with fibroblasts. The overarching goal of this work is to evaluate the cytotoxicity effect of ISMs of different compositions, which are the basis of ion sensing in many wearable and implantable devices. For this purpose, the membranes are evaluated in specific experimental conditions that mimic real operating scenarios, apart from the exploration of the responsible compound in case that any toxicity is detected. Furthermore, the ISMs were prepared in different configurations as according to whether they were part of ISEs of an inner-filling solution type or all-solid-state electrodes based on conventional drop-casting of the membrane, peeling after the preparation of a wearable sensor, and detachment from a microneedle-based sensor, thus covering a wide range of membrane shapes. Advantageously, different kinds of plasticizers and ionophores were tested in combination with assays that focus on the medium-term and long-term leaching of compounds. Apart from the demonstration of the biocompatibility of the different ISMs tested herein, we intend to create an awareness in the scientific community regarding the need to run biocompatibility assays during the very first steps of any sensor development. This will permit meeting the requirements for subsequent on-body application<sup>55</sup> and massive in vivo validations of the final commercialization of the device.

## MATERIALS AND METHODS

**Reagents, Materials, and Instrumentation.** Valinomycin (potassium ionophore I, selectophore grade), potassium ionophore II, calcium ionophore IV, nonactin (ammonium ionophore I), sodium

ionophore X, hydrogen chromoionophore I, sodium tetrakis[3,5-bis(trifluoromethyl)phenyl]borate (NaTFPB) with >98% purity, potassium tetrakis(4-chlorophenyl)borate (KTCIPB), bis(2-ethylhexyl)sebacate (DOS) with ≤97% purity, 2-nitrophenyl octyl ether (*o*-NPOE) with >99% purity, 2-fluorophenyl 2-nitrophenyl ether (FNDPE) (selectophore grade >98% purity), Poly(vinyl chloride) (PVC), tetrahydrofuran (THF), and multiwalled carbon nanotubes (MWCNTs) were purchased from Sigma-Aldrich. Polyurethane (PU) Tecoflex type SG80A was purchased in Tecoflex (see the [Supporting Information](#) for more details about this compound). Analytical-grade chloride salts of potassium and sodium were procured from Sigma-Aldrich. Aqueous solutions needed for potentiometric experiments were prepared in 18.2 MΩ cm<sup>-1</sup> doubly deionized water (Milli-Q water system, Merck Millipore).

In the potentiometric experiments, an electromotive force (EMF) was measured with a high input impedance (10<sup>15</sup> Ω) EMF16 multichannel data acquisition device (Lawson Laboratories, Inc.) against either a double-junction Ag/AgCl/sat. KCl/1 M LiOAc reference electrode (6.0726.100, Metrohm Nordic AB, Sweden). All experiments were carried out at room temperature (25 °C) and under constant stirring of 400 rpm (Stirrer; IKA Color Squid S000, IKA, Germany). Glassy carbon electrodes (6.1204.300 GC, Metrohm Nordic AB, Sweden) were connected to the potentiometer by a cable based on electrical clamps and BNC outputs.

**Table 1** presents the composition of all of the membrane cocktails prepared in THF for the cytotoxicity assays. In addition, for the preparation of the potassium-selective electrodes utilized in the potentiometric experiments, two different membranes were tested: (i) a cocktail mixture of 2 wt % valinomycin (18 mmol kg<sup>-1</sup>), NaTFPB (10 mmol kg<sup>-1</sup>), 33 wt % of PU and 65 wt % of DOS in 1 mL of THF,<sup>13,19</sup> and (ii) a cocktail based on 0.3 wt % KTCIPB, 1 wt % potassium ionophore II, 31.7 wt % PVC, and 67 wt % *o*-NPOE in 1 mL of THF.<sup>56</sup> A solution of 1 mg mL<sup>-1</sup> of MWCNTs functionalized (fMWCNTs according to Yuan et al.<sup>57</sup>) in ethanol was used to modify the commercial GC electrode (five layers of 10 μL deposited by drop-casting and waiting 5 min before depositing each layer). Finally, each of the two ISMs was deposited as five layers of 50 μL of the corresponding cocktail by drop-casting.

**Cytotoxicity Assays.** The cytotoxicity assays consisted of the evaluation of the toxic effects of the membranes presented in **Table 1** by cell counting with a MOXI Z mini automated cell counter kit



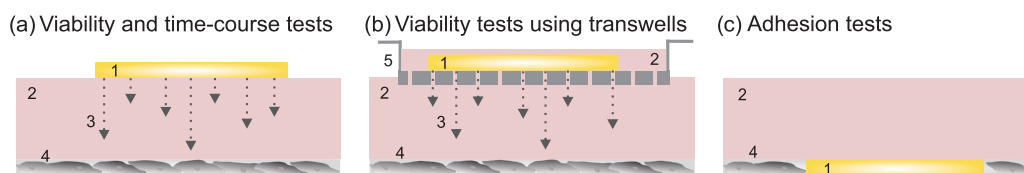


**Figure 2.** Illustration of the three different configurations used in the cytotoxicity assays: (a) direct placement of the ISM on top of the culture media where the cells are growing at the bottom of each well. This configuration was employed for the viability tests and time-course (or proliferation) tests; (b) use of a transwell scaffold for the deposition of the ISM to keep the ISM suspended in the culture media. This configuration was used in viability tests; and (c) deposition of the ISMs directly on the well before adding the culture cell to keep the ISM attached to the bottom of the well. This configuration was utilized in the adhesion tests. 1: ISM, 2: culture media, 3: arrows illustrating the possible leaching of the components of the ISM, 4: cells attached to the surface of the well in the monolayer disposition, 5: transwell.

(Orflo) after a certain incubation time of the human dermal fibroblast (HDF) (NHDF-Ad-human dermal fibroblast, adult, CC-2511, Lonza) cell culture in the presence of these membranes.

**Viability Tests without Transwells.** A total of 35,000 cells per well were seeded in a 24-well plate in Dulbecco's modified Eagle's medium (DMEM)-Glutamax + 10% fetal bovine serum (FBS heat-inactivated). These cells were left in the incubator to grow for approximately 72 h. A volume of 4  $\mu$ L of each type of membrane (Table 1) was drop-casted on a glass plate and left to dry for 4 h until the total evaporation of THF. Subsequently, these membranes were peeled off the glass plate and sterilized for 15 min under a UV lamp before adding them to the cell culture. The cells were fed with 1 mL of culture media (DMEM, high glucose, GlutaMAX Supplement, pyruvate, 10569010, ThermoFisher), and the membranes were located floating in the media and placed in each well with sterile tweezers. After 96 h of incubation with the membranes (adding media to the cells every 2 days), the cells were counted. This procedure was completed as follows: (i) the media and membrane were removed in each well; (ii) the cells were washed with 1 mL of Dulbecco's phosphate-buffered saline (DPBS) without Ca and  $Mg^{2+}$  (PBS<sup>-/-</sup>) per well; (iii) a volume of 350  $\mu$ L of trypsin was added to each well and placed in the incubator for 5 min to detach the cells; (iv) a volume of 700  $\mu$ L of the media was added to each well to stop further cell degradation; and (v) a volume of 75  $\mu$ L of cells was taken and injected into the MOXI chip.

**Viability Tests with Transwells.** A similar procedure was carried out in these experiments, but the membranes were deposited directly in the transwell. A volume of 4  $\mu$ L of the corresponding membrane cocktail (Table 1) was drop-casted on the bottom part of the transwell and left to dry for 24 h until the total evaporation of THF. The transwells containing the membranes were sterilized for 15 min under a UV lamp. Subsequently, the cells were fed with 700  $\mu$ L of culture media; then, the transwells were placed in each well, and a volume of 300  $\mu$ L of media was finally added to each transwell. The cells were cultured in the incubator for 5 days (feeding them with media every 48 h) and counted according to the same procedure described above for the experiments without transwell.

**Proliferation (Time-Course) Tests.** A total of 35,000 cells per well were seeded in six different plates (24-well plate) with DMEM-Glutamax + 10% FBS (heat-inactivated). The cells were incubated for 72 h before adding the membranes in the wells following the procedure described above. The cell culture was stopped at different time points in each plate, measuring cell numbers, as described above, 6, 24, 36, 48, 72, and 96 h after the membrane addition.

**Adhesion Tests.** The membranes were drop-casted into the empty wells of a 24-well plate, followed by a 15 min sterilization under UV lamp. Subsequently, 35,000 cells per well were seeded with DMEM-Glutamax + 10% FBS (heat-inactivated) and incubated for 48 h approximately. Then, the cells were fixed with 4% methanol-free formaldehyde at room temperature for 15 min to continue with the immunofluorescent staining.

The cells were permeabilized with 0.3% Triton X-100 in Dulbecco's phosphate-buffered saline (DPBS) for 10 min and blocked with 4% FBS and 0.1% Tween-20 in DPBS for 1 h. Primary antibodies were diluted in 4% FBS, 0.1% Tween-20, DPBS solution: caspase-3

(CASP3) (1:250, Cell Signaling, clone 8G10) and Ki67 (1:250, Cell Signaling, clone D3B5). The primary antibodies were then incubated overnight at 4  $^{\circ}$ C followed by 2 h of incubation at room temperature with Alexa Fluor 488 donkey anti-rabbit IgG secondary antibodies (1:1000, Life Technologies, R37118) diluted in 4% FBS, 0.1% Tween-20, DPBS solution. Nuclei were stained with Hoechst 33342 (fluorescent dye for labeling DNA) (1:1000, Invitrogen). Images were acquired with a Zeiss LSM710-NLO point scanning confocal microscope. Postacquisition analysis of the pictures was performed using ImageJ.

## RESULTS AND DISCUSSION

Herein are presented a series of cytotoxicity assays based on viability, proliferation, and adhesion tests using human fibroblasts in a culture media within which different ISMs are placed. Essentially, a piece of the tested material is present while the cells are cultured under well-established conditions of incubation (see the [Materials and Methods](#) section for more details). Then, the assay performed consists of the observation of morphological changes and/or variations in the number of cells compared with control experiments without the material under study. This method was described as highly sensitive and convenient for low-density materials, such as ISMs.<sup>5</sup> During the incubation of the cells, any compound leaching from the material is able to diffuse through the culture media, therefore contacting the cell monolayer at the bottom of the well. On the other hand, the ISM may be exposed to the cell monolayer during the so-called adhesion experiments. Any reactivity (toxicity) of the tested sample is indicated by proliferation abnormalities, degeneration, and/or death of the cells in their surroundings, i.e., the variation of the number of cells after incubation.

It is important to highlight certain characteristics of the cell line used in this study to further provide a trustworthy interpretation of the observations. The human diploid fibroblasts, also referred to as human dermal fibroblasts (HDFs), have a defined replicative life span. Thus, the mean cell cycle time is proportional to the replicative age in terms of mass culture and clones.<sup>58</sup> Importantly, its replicative cycle may be altered in the presence of different materials. For example, with a low serum concentration, the replicative potential decreases, whereas it can be increased using epidermal growth factor (EGF) or other stimulants, such as glucocorticoids.<sup>59</sup> In this latter case, the average time of the replicative cycle is between 20.7 and 28.7 h depending on whether some EGF was added to the culture media or not, respectively.<sup>58,59</sup>

Three different in vitro assays employing HDF were carried out in our studies to evaluate the cytotoxicity of traditional ISMs, as illustrated in [Figure 2](#). For the viability tests, either the direct placement of the ISM floating on top of the culture

media (Figure 2a) or on the bottom part of transwell (Figure 2b) was tested. In the latter case, the ISM is maintained on top of the well while being immersed in the cell culture media. The same kind of setup as in Figure 2a was used for the proliferation tests, whereas adhesion studies were conducted by depositing the ISM directly on the bottom of the well and later adding HDFs and the corresponding culture media (Figure 2c).

**Cell Viability Tests.** First, a screening of the most widely used cation receptors (also referred to as ionophores) and plasticizers in the preparation of ISMs was performed by means of cell viability tests at 96 h of cell incubation. A total number of 11 conditions were tested by triplicates, including a control condition (monolayer of fibroblasts immersed in culture media and without the presence of any membrane); membranes based on the cation exchanger NaTFPB in PU/DOS matrix without (membrane I) and with MWCNTs (membrane II); membranes based on NaTFPB, PU, as well as *o*-NPOE or FNDPE as plasticizer (membranes III and IV, respectively); membranes comprising NaTFPB, PU, DOS, and different ionophores [potassium ionophore I (membrane V), ammonium ionophore I (membrane VI), calcium ionophore IV (membrane VII), sodium ionophore X (membrane VIII), hydrogen chromoionophore I (membrane IX), and potassium ionophore II (membrane X)].

At this point, it is important to clarify two issues related to the tested membranes. First, regarding the selection of ammonium ionophore I (also called nonactin), while we are aware of the problematic of potassium interference in physiological conditions ( $\log k_{\text{NH}_4\text{K}} = -0.9$ ),<sup>60</sup> there are some wearable devices that use this ionophore in the preparation of ammonium-selective electrodes for sweat analysis reported by worldwide-recognized groups working on this topic.<sup>60–62</sup> This is the reason for the exploration of this ionophore in our studies.

Then, concerning the use of PU as polymeric matrix, while PVC is the polymer most widely used in the preparation of ISMs, PU is gaining momentum in the preparation of wearable and implantable sensors because of its improved bio- and hemocompatibilities, better adherence with the majority of electrode substrates, and its higher flexibility, among other advantages.<sup>1,63,64</sup> Importantly, in our previous work about microneedle-based sensors,<sup>19</sup> we compared PVC- and PU-based membranes comprising valinomycin as proof-of-concept and did not detect any difference in cell viability studies. It was therefore concluded that, at the time frame of the experiments based on the 24 h replicative cycle of the cells, the polymeric matrix seems to not influence the experimental observations.

Figure 3 depicts the outcomes for the viability testing given as the percentage of the counted number of cells in each condition with respect to the control. In addition, a comparison of the same experiment accomplished without and with transwell (see the setups illustrated in Figure 2a,b respectively) and with the viability expressed as the raw cell number is presented in Figure S1 (Supporting Information). As expected, the trend observed for each condition was exactly the same without and with transwell, with the peculiarity that the presence of the transwell decreased the total number of cells counted after the 96 h of incubation (see the control condition in Figure S1). Consequently, any difference found between the cases without and with transwell is based on this effect, thereby negating the different viabilities of the tested

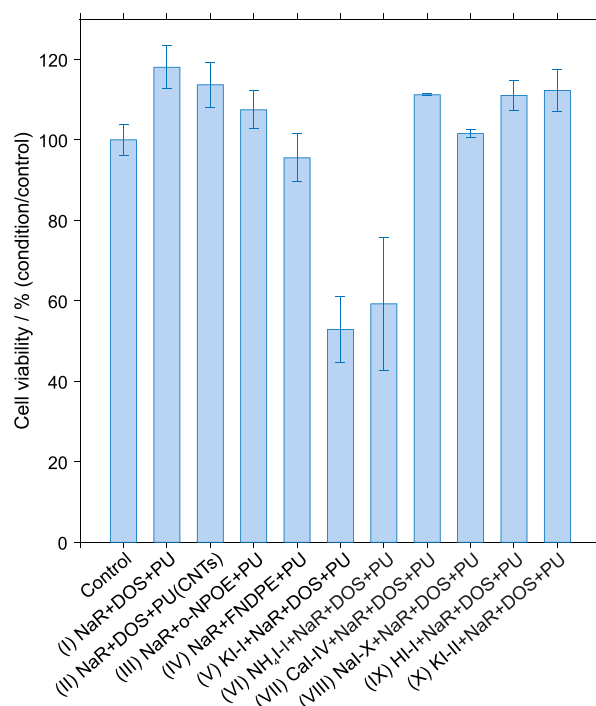


**Figure 3.** Cell viability assays in the presence of different ISMs for HDF incubation of 96 h. Viability percentage was calculated from the total number of cells counted in each condition with respect to the control. PU: polyurethane; NaR: cation exchanger; DOS: dioctyl sebacate; *o*-NPOE: 2-nitrophenyl octyl ether; CNTs: carbon nanotubes; FNDPE: 2-fluorophenyl 2-nitrophenyl ether; KI-I: potassium ionophore I (valinomycin); NH<sub>4</sub>I-I: ammonium ionophore I (nonactin); CaI-IV: calcium ionophore IV; NaI-X: sodium ionophore X; HI-I: chromoionophore I; and KI-II: potassium ionophore II (mutacin). The number of the membrane, as labeled in Table 1, is given in parentheses.

ISM. From this point, all of the observations discussed in the present paper are based on in vitro experiments without the use of transwells.

Regarding the different membranes, all of them had roughly the same number of cells as the control condition with the major exceptions of membranes V and VI based on potassium ionophore I and ammonium ionophore I ( $52.8 \pm 8.2$  and  $59.3 \pm 16.4\%$  of cell viability, respectively). This outcome revealed that under the selected experimental conditions, only two compounds, specifically valinomycin (potassium ionophore I) and nonactin (ammonium ionophore I), of all of those employed with the different membranes show cytotoxic effects in the time frame tested (long-term incubation of 96 h) of the HDF. Furthermore, the observed toxicity was a consequence of the compound leaching from the ISM (i.e., gradual dissolution into the culture media) as this is the most likely mechanism for the ISM components to reach the monolayer of the HDF at the bottom of the well (see Figure 2a,b).

Importantly, the leaching of the ionophore from the membrane is commonly quantified by its lipophilicity ( $\log P_{\text{TLC}}$  as the logarithm of the partition coefficient between 1-octanol and water as estimated experimentally by the use of thin-layer chromatography).<sup>65</sup> As a general behavior, when the ionophore presents  $\log P_{\text{TLC}} < 6$ , the leaching roughly starts after 2–3 days of the membrane preparation and in continuous contact with an aqueous medium.<sup>66</sup> Concerning the tested ionophores, the lowest lipophilicity corresponds to potassium

ionophore I ( $\log P_{\text{TLC}} = 7.8$ ) and ammonium ionophore I ( $\log P_{\text{TLC}} = 5.8$ ), coinciding with the two compounds found to present certain toxicity in our experiments (Figure 3), while the rest of ionophores are considered highly lipophilic with  $\log P_{\text{TLC}} > 8$ .<sup>67,68</sup>

Even though the interpretation of the cytotoxicity observations may be associated with a higher leaching rate of potassium ionophore I and ammonium ionophore I from the membrane to the cell culture media, it is not discharged that the rest of ionophores may present certain toxicity at longer experimental times. What is evident from our results is that the use of membranes containing potassium ionophore I and ammonium ionophore I is not convenient at the selected conditions, while the rest of compounds (PU, f-MWCNTs, plasticizers, and other ionophores) did not manifest any cytotoxicity effects.

It is worth mentioning that in the majority of the tested membranes, there was an increase in the counted number of cells with respect to the control (see Figure S1, Supporting Information). However, this increase was not high enough to suspect mutagenesis events, and further experiments would be required to investigate a possible mechanism of action or to discard a random variability occurring during the cell seeding and counting. Indeed, it is here anticipated that the immunostaining measurements with these two membranes did not exhibit a higher presence of the proliferation biomarker (Ki67) in the cell adhesion studies shown below.

Evaluating now the membrane II (containing f-MWCNTs), while adverse effects have been demonstrated following respiratory exposure depending on the composition and size of the CNTs,<sup>9</sup> no effect was determined in our studies in terms of cell death or proliferation. This is probably because of the absence of f-MWCNTs leaching from the membrane into the solution. Notably, the selected amount of f-MWCNTs with respect to the rest of the ISM components was really high to mimic any possible presence of this material in the membrane phase of all-solid-state ISEs comprising a layer of this material as an ion-to-electron transducer.<sup>57</sup>

Finally, the standard deviation found for the replicates of the viability results (see error bars in Figures 3 and S1) is a result of the variability inherent to any step of the experiments, from the membrane deposition on the glass plate to cell seeding, washing, and/or counting. Relative standard deviations were always lower than the 20%, which here is accepted as within the tolerance level for a qualitative study, apart from the case of the nonactin-based membrane that was close to the 40%, likely because of the toxic effect of the compound per se. In addition, to confirm our qualitative interpretation of the observations in all of the *in vitro* tests presented through this paper, we have accomplished a statistical analysis of the data (i.e., analysis of variance: two-factor without replication and *t*-test: paired two samples for means); see the Supporting Information and Table S1.

### Cell Proliferation Tests or Time-Course Experiments.

As viability assays demonstrated the cytotoxicity of valinomycin and nonactin in HDF, most likely, through the leaching of these compounds from the ISM to the culture media under the long-term exposure of 96 h, we subsequently conducted a time-course experiment to study the leaching (and therefore the initiation of the toxic effects) in a shorter time frame. For this purpose, HDF cells were maintained in culture for 3 days until reaching a confluent stage, and after that, the membranes were placed floating in the cell media. The ISMs were prepared

as detailed in the Materials and Methods section, by drop-casting a volume of 4  $\mu\text{L}$  of the cocktail in the glass plate. Then, cell proliferation was evaluated within different time frames (6, 24, 36, 48, 72, and 96 h) according to its own control (without any ISM, just the HDF monolayer + culture media).

Figure 4a features the results observed in these experiments. It is evident that both ionophores displayed the same trend, where a decrease in cell numbers was found from 36 h of incubation onwards. Because the replicative cycle of HDF is around 24 h, this decrease could be indicative of an effect during the second cycle produced by leaching of the compound from the membrane started between 24 and 36 h during the incubation. In addition, in the case of the nonactin-based membrane, the cells exhibited greater formation of vacuoles (see Figure S2 in Supporting Information). This is a feature that potentially points out a different mechanism of action in comparison with the cells in contact with the valinomycin-based membrane. Furthermore, it is here anticipated that the immunostaining performed on cell adhesion studies for these two compounds did not show notable differences of the two biomarkers tested, showing positive results for proliferation (Ki67) and negative for apoptosis (CASP3). Because higher toxicity of nonactin compared to that of valinomycin has been previously reported,<sup>69</sup> further experiments with other biomarkers would be required to fully understand the different mechanism of action.

Two variables that may influence the leaching process of ISMs, as well as its time frame, were also studied as follows: (i) the conformation of the membrane and (ii) the plasticizer used in the membrane matrix. Figure 4b depicts the results for the time-course experiments involving ISMs based on valinomycin and with different configurations: i.e., for an electrode based on inner-filling solution (membrane XI), membrane detached from a modified microneedle (membrane V)<sup>19</sup> or from a wearable patch (WPIS, membrane V)<sup>13</sup> and a membrane prepared by direct drop-casting on the glass plate (membrane V). Whereas a decrease in cell numbers (%) was seen for all cases, this started at 24 h for the membrane typically used in inner-filling solution electrodes and at 36 h for the rest.

Considering now the patterns displayed during the time frame 36–96 h, the toxicity order of the different conformations may be roughly established as inner-filling solution > drop-casted  $\geq$  WPIS > microneedle. Yet, overall, the main outcome was the pronounced toxicity of the membrane for the inner-filling solution electrode. This finding is likely illustrated by the higher content of valinomycin in this membrane in comparison with the rest of the configurations ( $1.5 \times 10^{-7}$  mol for the membrane with the inner-filling solution configuration vs  $7.2 \times 10^{-9}$  mol for the rest). Thus, considering that cytotoxicity's appearance depends on the compound leaching (i.e., its partition between the membrane and the cell culture media phases), its presence in the cell culture media will increase with the initial amount in the membrane and therefore cytotoxicity will be detected sooner. In other words, the membrane cytotoxicity is dose-dependent with respect to valinomycin. Most likely, this behavior is extended to the rest of ionophores.

Regarding valinomycin-based membranes prepared with various plasticizers, i.e., DOS (membrane V in Table 1), *o*-NPOE (membrane XII), and FNDPE (membrane XIII) with the same wt % (Figure 4c), similar trends were apparent for all



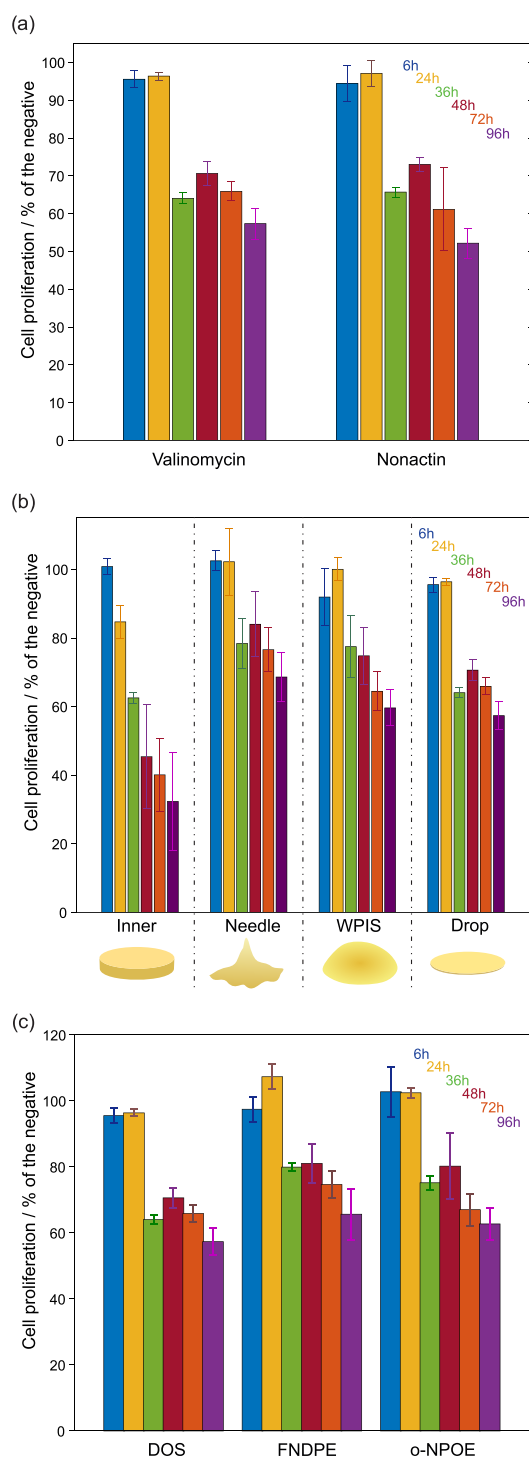


**Figure 4.** Time-course viability assays. (a) Membranes V and VI comprising valinomycin and nonactin at different time frames of 6, 24, 36, 48, 72, and 96 h. (b) Membranes based on valinomycin that were prepared with various conformations, i.e., for an electrode based on inner-filling solution (XI), detached from a modified microneedle (V) or wearable (WPIS, V) and prepared by direct drop-casting in the glass plate (V). (c) Membranes comprising valinomycin and different plasticizers: DOS (V), *o*-NPOE (XII), and FNDPE (XIII). Viability percentage was calculated from the total number of cells counted in each condition with respect to the control. PU: polyurethane; NaR: cation exchanger; DOS: dioctyl sebacate; *o*-NPOE: 2-nitrophenyl octyl ether; FNDPE: 2-fluorophenyl 2-nitrophenyl ether.

cases, i.e., toxicity from 36 h onwards. It may be hypothesized that more leaching of the ionophore occurs in the following order: DOS > *o*-NPOE > FNDPE, coinciding with the order of the dielectric constants for these plasticizers (4, 24, and 50, respectively).<sup>70</sup> Despite the fact that it is known that the plasticizer's nature influences the flexibility and softness of the ISMs, as well as the physical entrapment of the other components,<sup>40</sup> the differences observed in our proliferation experiments for each plasticizer were not disparate enough to establish a general conclusion. Indeed, whether different leaching is manifested with the change of the plasticizer, this would probably occur in a time frame shorter than the replicative life span of the HDF (22 h approximately), and, therefore, this would not be detected during the present *in vitro* cytotoxicity experiments.

**Cell Adhesion Assays.** The growth capability of the HDFs in the surroundings of the ISMs was additionally determined to evaluate the invasiveness level of all materials, specifically according to the setup displayed in Figure 2c. Notably, in all of the experiments presented till date, the ISM compound could reach the HDF monolayer only after leaching from the membrane to the culture media (Figure 2a,b). Conversely, in the adhesion experiments, the cells were directly seeded on top of the ISM, aiming at mimicking the contact of the sensor with living tissues. Note that, in these experiments, cytotoxicity coming from compounds' leaching is evidently possible.

Along these lines, there are not many studies in the literature that comprise the evaluation of electrochemical sensors by means of analogous experiments. For example, Miller and co-workers studied the interaction of microneedle-based electrodes (amperometric sensors for the detection of glucose and lactate) with macrophages at 2 and 24 h, reporting the need of a cell-resistant (Lipidure) coating to inhibit macrophage adhesion.<sup>17</sup> In other works, Espadas-Torre and Meyerhoff demonstrated that polymeric membranes exhibited thrombogenic properties during *in vitro* platelet adhesion studies.<sup>26</sup>

Importantly, cell adhesion on the sensor surface may affect electroanalytical performance, such as blocking the mass transfer of analytes toward the surface, along with the rise in adverse effects appearing in the patient.<sup>26,71</sup> To avoid cell adhesion, therefore improving the biocompatibility of the sensor, some researchers have proposed the use of conventional dialysis membranes or hydrogel layers as outer overlays.<sup>25</sup> Nevertheless, these solutions lead to worsening both sensitivity and response time.<sup>26</sup> In the case of medical devices based on subcutaneous sensors, Lindner and co-workers showed that the inflammatory response decreased by reducing the plasticizer content in the ISM.<sup>71</sup>

As the composition of the ISM seems to drastically affect the biocompatibility of the sensors in terms of cell adhesion, we studied the following cases: (i) membranes for which components were incorporated one by one {PU (membrane XIV), PU + ion exchanger (membrane XV), PU + ion exchanger + DOS at different PU/DOS ratios (1:2 [membrane I], 1:1 [membrane XVI], and 2:1 [membrane XVII])}; (ii) membranes with different plasticizers [DOS, NPOE, and FNDPE; membranes I, III, and IV, respectively]; (iii) membranes comprising different ionophores with previously confirmed toxicity in viability tests [valinomycin (membrane V) and nonactin (membrane VI)] and ionophores with already demonstrated nontoxicity in the viability tests [potassium ionophore II (membrane X) and sodium ionophore X (membrane VIII)]. In addition, it is expected that ISM

conformation may also have an influence on cell adhesion. Accordingly, two different conformations of the membranes, membrane V and membrane XI, based on valinomycin, i.e., direct drop-casting in the well or a piece of the membrane for the inner-filling solution electrodes, were tested.

Figure 5 portrays the results obtained through the adhesion tests by depositing the corresponding ISM at the bottom of the

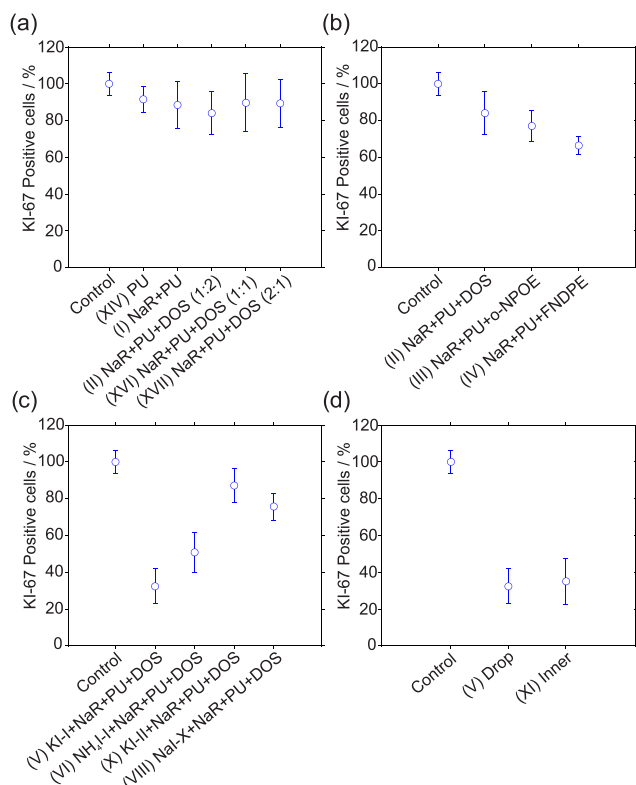


**Figure 5.** Adhesion test showing the percentage of the proliferation of cells with the biomarker, Ki67, with respect to the control condition (no additional material in the cell culture media). (a) Membranes prepared including the components one by one: PU (XIV), PU + cation exchanger (XV), PU + cation exchanger + DOS at different PU/DOS ratios (1:2 I, 1:1 XVI, and 2:1 XVII). (b) Membranes based on different plasticizers: DOS, NPOE, and FNDPE, I, III, and IV, respectively. (c) Membranes based on different ionophores valinomycin (V), nonactin (VI), potassium ionophore II (X), and sodium ionophore X (VIII). (d) Membrane V comprising valinomycin with two different conformations. The number of the membrane, as labeled in Table 1, is given in parentheses.

well (unless for the membrane refers to the inner-filling solution electrode that was placed there after peeling off from the glass plate) and, subsequently, adding the HDFs and culture media (Figure 2c). Importantly, the fibroblasts, and most of the cell lines excepting the hematopoietic cells, are anchorage-dependent, which means they tend to attach first to the substrate and proliferate, performing a monolayer at the bottom of the well surface.<sup>8,72</sup> The nuclear marker Ki67 highlights proliferating; thereby, a decrease in the number of Ki67+ cells can be interpreted as an effect on any of the mechanisms involved in the proliferation process. Considering this information, the interpretation of the results in Figure 5 is as follows.

First, PU, DOS, and the ion exchanger (i.e., NaTFPB) did not inhibit the proliferation of fibroblasts (Figure 5a). Second,

there is a reduction in the number of Ki67+ cells in the order: DOS > *o*-NPOE > FNDPE (Figure 5b). While the membranes comprising DOS or *o*-NPOE presented only a slight decrease with respect to the control ( $84.0 \pm 11.8$  and  $77.0 \pm 8.6\%$ , respectively), it is evident that FNDPE was the most toxic when the cells were exposed to this membrane ( $66.4 \pm 4.7\%$ ). Third, the toxic effect of valinomycin (membrane V) and nonactin (membrane VI) was again manifested with a % of Ki67+ cells of  $32.4 \pm 9.5$  and  $50.8 \pm 10.8\%$ , respectively, against percentages of  $87.2 \pm 9.1$  and  $75.5 \pm 7.4\%$  for potassium ionophore II (membrane X) and sodium ionophore X (membrane VIII), respectively (Figure 5c). Finally, the valinomycin-based membrane had the same results for the biomarker ( $32.4 \pm 9.5$  and  $35.1 \pm 12.5\%$  for the drop-casted membrane and the piece of the inner-filling solution membrane, respectively), regardless of membrane conformation (Figure 5d).

Assuming that values below 85% are indicative of a toxic effect in the corresponding cell adhesion experiment, it can be concluded that membranes based on FNDPE (plasticizer), or valinomycin and nonactin (ionophores) exhibit cytotoxicity showing the first effects after 36 h of exposure. Consequently, these materials are not classified as suitable for the preparation of transdermal and implantable sensors because they present cytotoxicity in the different conditions tested.

Figure 6 presents the immunofluorescence images of the adhesion tests corresponding to the proliferation behavior of

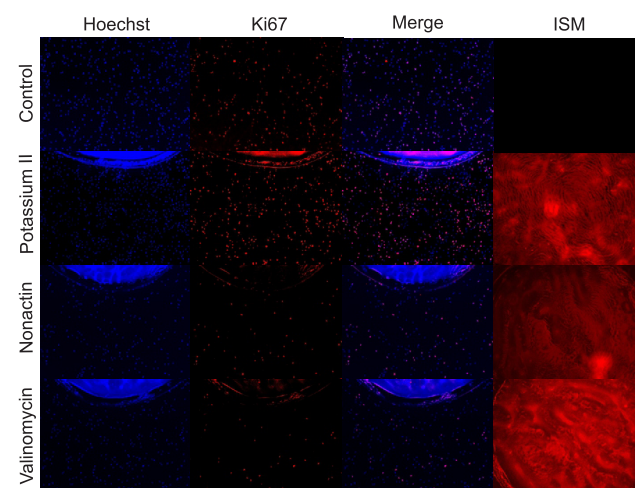


**Figure 6.** Immunofluorescence images from adhesion tests showing (in columns) the total number of cells (Hoechst 33342), cells under proliferation (Ki67), the merger of both Hoechst 33342 and Ki67, as well as the ISM drop-casted on the surface of the 24-well plate (the negative control does not have any membrane deposited, and a black chart is presented instead). The rows feature the different tested conditions: the negative control, ISM based on potassium ionophore II (membrane X), nonactin (VI), and valinomycin (V). ISM = ion-selective membrane.

the cells in the presence of ISMs based on the different ionophores. Two different biomarkers have been used in this assay: Ki67 as a proliferation marker and CASP3 as an apoptosis marker. Additionally, Hoechst 33342 has been used to stain the nuclei allowing total cell number counting. As observed, there was a dramatic decrease in the total number of cells for the ISMs based on valinomycin and nonactin, shown by Hoechst staining, in comparison with the negative control



and the nontoxic potassium ionophore II (membrane X). This decrease can be explained by an inhibition of the proliferation, shown by a reduction on the number of Ki67+ cells, thereby revealing the adverse effect that these toxic ionophores can produce in the division of the fibroblasts. The fact that no CASP3+ cells were found in any of the tested ISMs (data not included for simplicity) reinforces the hypothesis that the reduction in cell numbers is due to an inhibition of the proliferation rather than an induction of apoptosis. Nevertheless, further experiments would be required to rule out different mechanisms of action for cell death. Finally, very few cells were encountered on top of the ISMs (see the last column in Figure 6), indicating that HDFs do not attach or grow on the top of the ISMs.

**Potentiometric Response of Ion-Selective Membranes with Critical Compositions from a Biocompatibility Perspective.** Having inspected the potential cytotoxicity of ISMs, it is clear that there is an incompatibility when using nonactin and valinomycin as ionophores, as well as FNDPE as a plasticizer in ISMs for more than 24–36 h. We subsequently explored alternatives to these materials for utilization in ISMs while distorting the least possible the analytical performance offered by these compounds.

Nonactin is the ammonium ionophore employed per excellence in ISMs, and this receptor and chromoionophore III (ETH5350), which is a phenoxazine derivative,<sup>73</sup> are the only two commercially available ionophores for ammonium to the best of our knowledge. Bearing in mind the cytotoxicity presented by nonactin, chromoionophore III could be an alternative for ion sensors, but it suffers from strong interference by Na<sup>+</sup> and K<sup>+</sup> ions. This will limit the application of the corresponding ISE in any biological fluid. The other option is the use of other synthetic ammonium receptors acting through hydrogen bonds, electrostatic and/or cation- $\pi$  interactions, hydrophobic interactions, or reversible covalent-bond formation.<sup>74,75</sup>

In the case of potassium, it is herein demonstrated that the potassium ionophore II (mutacin, membrane X) does not exhibit any toxic effect on viability, proliferation, or adhesion during in vitro assays. As a result, we explored the analytical performance (i.e., in terms of calibration graph and selectivity) of ISMs based on this ionophore to be proposed as an alternative when developing wearable and implantable sensors for potassium analysis. Notably, the activity coefficients were calculated using a two-parameter Debye–Hückel approximation from the experimental concentrations.<sup>76</sup> Each logarithmic activity in the sample solution was plotted against the corresponding steady-state potential of the electrode, and the data were fitted to the Nernst equation as reported elsewhere.<sup>77</sup> The selectivity coefficients were calculated by the separate solution method through independent calibration curves first with the main interferent (i.e., Na<sup>+</sup> ions) and then the ion analyte after the electrode was conditioned in 1 mM solution of the corresponding cation.<sup>78–80</sup>

Figure 7 depicts the dynamic responses and corresponding calibration graphs for all-solid-state potentiometric ISEs comprising valinomycin or mutacin as potassium ionophore toward increasing concentrations of potassium in the sample solution. Both electrodes displayed a rapid response toward increasing potassium concentrations (10–30 s) with Nernstian slopes  $59.38 \pm 0.05$  and  $54.52 \pm 0.22$  mV for three electrodes based on valinomycin and mutacin, respectively. However, the mutacin-based sensor presented a reduced linear range of

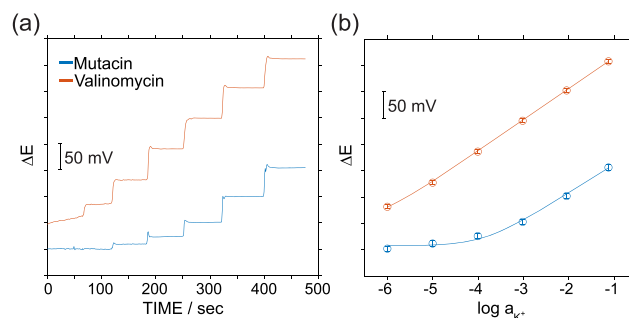


**Figure 7.** (a) Dynamic curves determined at increasing concentrations of potassium and (b) corresponding calibration graphs for valinomycin-based and mutacin-based ISMs.

response (LRR from  $10^{-3}$  to  $10^{-1}$  expressed in potassium activity) and a higher limit of detection (LOD of  $10^{-3.9}$  expressed in potassium activity) in comparison with the valinomycin-based electrode (LRR from  $10^{-5}$  to  $10^{-1}$  and LOD of  $10^{-6.2}$ ). Furthermore, a strong interference of Na<sup>+</sup> cations was observed according to the calculated logarithmic selectivity coefficients ( $\log K_{K,Na} = -0.75 \pm 0.06$  against  $\log K_{K,Na} = -4.20 \pm 0.52$  for mutacin and valinomycin, respectively). This selectivity is not suitable for the application of the sensor in biological fluids in which the analysis of potassium concentration will be totally masked by the presence of sodium ions.

It is worth mentioning that the membrane composition used for this study was the same as in the in vitro cytotoxicity assays, i.e., membrane X comprising PU, DOS, NaTFPB, and the ionophore. However, this is not the optimal composition reported for mutacin-based membranes, mainly in terms of selectivity. Thus, the logarithmic selectivity coefficient ( $\log_{K,Na}$ ) reported by Kimura and co-workers,<sup>81,82</sup> as well as Moody et al.,<sup>56</sup> was close to  $-3$  units. It is important to note that while the composition of the last mutacin-based membrane was different, the concentration of mutacin was the same as the previously used. Furthermore, all of the components for membrane preparation have been previously tested in cytotoxicity experiments, demonstrating the nontoxic effect toward the cells. When the membrane composition proposed by Moody et al. was used in our all-solid-state electrodes (i.e., 0.3 wt % KTCIPB, 1 wt % potassium ionophore II, 31.7 wt % PVC, and 67 wt % *o*-NPOE in 1 mL of THF), an improved selectivity coefficient was observed ( $\log_{K,Na} = -3.2$ ) while observing a fast response time (20 s), Nernstian response ( $-60.5 \pm 0.8$  mV), as well as LRR and LOD ( $10^{-6}$ – $10^{-1}$  and  $10^{-6.9}$ , respectively) suitable for potassium detection in sweat (clinical range of 4–24 mM),<sup>1,83</sup> blood (3.5–5.3 mM),<sup>84–86</sup> and urine (25–125 mM day<sup>-1</sup>).<sup>86,87</sup> Advantageously, the calculated selectivity coefficient is, in principle, suitable for measuring a low amount of potassium in the presence of a high amount of sodium. For example, in the case of sweat, the common concentration ranges are 4–24 and 20–100 mM for potassium and sodium, respectively, which involves the need of selectivity coefficients in the range of  $\log K_{K,Na} = -0.9$  to  $-2.5$  for the effective analytical detection of potassium. Consequently, mutacin may be recommended as an ionophore in wearable, transdermal, and implantable potassium sensors.

It is important to mention that, even though this membrane composition was not tested in the present cell viability studies, no cytotoxic effect is expected on the basis of our previous results that compared PVC- and PU-based membranes

comprising valinomycin as ionophore.<sup>19</sup> Thus, at the time frame of the experiments based on the 24 h replicative cycle of the cells, the polymeric matrix seems to not influence the experimental observations. This conclusion may also be extended to membranes based on potassium ionophore II, which indeed presents higher lipophilicity ( $\log P_{\text{TLC}} = 7.8$  vs  $\log P_{\text{TLC}} = 10.7$  for valinomycin and potassium ionophore II, respectively).<sup>67</sup>

Finally, to avoid the use of FNDPE as the plasticizer, there is a large palette of plasticizers to utilize instead. The only reason one would use FNDPE would be to reduce the leaching of ISM compounds into the solution, therefore mitigating any possible toxic effects emanating from this process. However, when we tested the performance of potentiometric ISEs comprising valinomycin-based membranes with DOS, o-NPOE, and FNDPE as the plasticizer, we did not detect any difference in calibration parameters (see slope, LOD, and LRR in Table S2 and Figure S3, Supporting Information). So, the substitution of FNDPE with another plasticizer is possible; indeed, this is not the most widely employed plasticizer for the general preparation of ISMs.

## CONCLUSIONS

We assessed the toxicity of the most widely used compounds to fabricate ISMs for potentiometric ISEs. For this purpose, different experiments based on in vitro viability, proliferation, and cell adhesion assays were carried out using human fibroblasts and ISMs of different compositions and conformations. The viability results revealed that valinomycin (potassium ionophore) and nonactin (ammonium ionophore) are to a large extent toxic for fibroblasts after leaching from the membrane into the culture media. This effect is mainly produced by an inhibition of the proliferation rate of the cells rather than yielded by apoptosis, although other cell death mechanisms cannot be ruled out. Time-course (or proliferation) experiments demonstrated that the toxic impact of valinomycin and nonactin begins between 24 and 36 h of cell incubation, likely connected to more marked leaching of the compounds over this time frame. These two compounds, as well as the plasticizer (FNDPE), showed additional toxicity when the fibroblast monolayer was exposed to the membranes during cell adhesion tests. Potentiometric ISEs based on mutacin as a potassium ionophore were evaluated as an alternative to the use of valinomycin as mutacin is not toxic in any of the variants presented in our studies. Advantageously, both ionophores had similar performances; therefore, mutacin may be used in the development of further biocompatible ISEs for potassium analysis in biological fluids. Herein, it is encouraged that there is the use of cytotoxicity assays during the very first steps of any sensor development with an intended biomedical application.

## ASSOCIATED CONTENT

### Supporting Information

The Supporting Information is available free of charge on the ACS Publications website at DOI: 10.1021/acssensors.9b01322.

Summary of the statistical analysis (Table S1); analytical performances of the electrodes (Table S2); cell viability assays with and without transwells (Figure S1); optical images of the control growing cells (Figure S2); and

dynamic responses and corresponding calibration graphs (Figure S3) (PDF)

## AUTHOR INFORMATION

### Corresponding Author

\*E-mail: gacp@kth.se.

### ORCID

Rocío Cánovas: 0000-0001-9552-535X

Marc Parrilla: 0000-0002-1344-8432

María Cuartero: 0000-0002-3858-8466

Gastón A. Crespo: 0000-0002-1221-3906

### Notes

The authors declare no competing financial interest.

## ACKNOWLEDGMENTS

The authors acknowledge the financial support of the KTH Royal Institute of Technology (Starting Grant Programme, K-2017-0371) and the Swedish Research Council (Project Grant VR-2017-4887). This project has received funding from the European Union's Horizon 2020 research and innovation programme under the Marie Skłodowska-Curie grant agreement 792824. R.C. thanks the Alfonso Martin Escudero Foundation.

## REFERENCES

- (1) Parrilla, M.; Cuartero, M.; Crespo, G. A. Wearable Potentiometric Ion Sensors. *TrAC, Trends Anal. Chem.* **2019**, *110*, 303–320.
- (2) Cuartero, M.; Parrilla, M.; Crespo, G. A. Wearable Potentiometric Sensors for Medical Applications. *Sensors* **2019**, *19*, No. 363.
- (3) Wang, S.; Lifson, M. A.; Inci, F.; Liang, L. G.; Sheng, Y. F.; Demirci, U. Advances in Addressing Technical Challenges of Point-of-Care Diagnostics in Resource-Limited Settings. *Expert Rev. Mol. Diagn.* **2016**, *16*, 449–459.
- (4) Vert, M.; Doi, Y.; Hellwich, K.; Hess, M.; Hodge, P.; Kubisa, P.; Rinaudo, M.; Schué, F. Terminology for Biorelated Polymers and Applications (IUPAC Recommendations 2012). *Pure Appl. Chem.* **2012**, *84*, 377–410.
- (5) Li, W.; Zhou, J.; Xu, Y. Study of the in Vitro Cytotoxicity Testing of Medical Devices. *Biomed. Rep.* **2015**, *3*, 617–620.
- (6) Hanks, C. T.; Wataha, J. C.; Sun, Z. In Vitro Models of Biocompatibility: A Review. *Dent. Mater.* **1996**, *12*, 186–193.
- (7) Bettazzi, F.; Palchetti, I. Nanotoxicity Assessment: A Challenging Application for Cutting Edge Electroanalytical Tools. *Anal. Chim. Acta* **2019**, *1072*, 61–74.
- (8) Babich, H.; Borenfreund, E. Cytotoxicity and Genotoxicity Assays with Cultured Fish Cells: A Review. *Toxicol. In Vitro* **1991**, *5*, 91–100.
- (9) Li, X.; Lee, S. C.; Zhang, S.; Akasaka, T. Biocompatibility and Toxicity of Nanoparticles and Nanotubes. *J. Nanomater.* **2012**, *2012*, 1–19.
- (10) Strangeways, T. S. P.; Fell, H. B. Experimental Studies on the Differentiation of Embryonic Tissues Growing in Vivo and in Vitro. I. The Development of the Undifferentiated Limb-Bud (a) When Subcutaneously Grafted into the Post-Embryonic Chick and (b) When Cultivated in Vitro. *Proc. R. Soc. B* **1926**, *99*, 340–366.
- (11) Khalili Fard, J. K.; Jafari, S.; Eghbal, M. A. A Review of Molecular Mechanisms Involved in Toxicity of Nanoparticles. *Adv. Pharm. Bull.* **2015**, *5*, 447–454.
- (12) Parrilla, M.; Ferro, J.; Guinovart, T.; Andrade, F. J. Wearable Potentiometric Sensors Based on Commercial Carbon Fibres for Monitoring Sodium in Sweat. *Electroanalysis* **2016**, *28*, 1267–1275.
- (13) Parrilla, M.; Ortiz-Gómez, I.; Cánovas, R.; Salinas-Castillo, A.; Cuartero, M.; Crespo, G. A. Wearable Potentiometric Ion Patch for

On-Body Electrolyte Monitoring in Sweat: Towards a Validation Strategy to Ensure Physiological Relevance. *Anal. Chem.* **2019**, 8644–865.

(14) Garcia, S. O.; Ulyanova, Y. V.; Figueroa-Teran, R.; Bhatt, K. H.; Singhal, S.; Atanassov, P. Wearable Sensor System Powered by a Biofuel Cell for Detection of Lactate Levels in Sweat. *ECS J. Solid State Sci. Technol.* **2016**, 5, M3075–M3081.

(15) Invernale, M.; Tang, B. C.; York, R. L.; Le, L.; Hou, D. Y.; Anderson, D. G. Microneedle Electrodes Toward an Amperometric Glucose-Sensing Smart Patch. *Adv. Healthcare Mater* **2014**, 3, 338–342.

(16) Valdés-Ramírez, G.; Li, Y. C.; Kim, J.; Jia, W.; Bandodkar, A. J.; Nuñez-Flores, R.; Miller, P. R.; Wu, S. Y.; Narayan, R.; Windmiller, J. R.; et al. Microneedle-Based Self-Powered Glucose Sensor. *Electrochem. Commun.* **2014**, 47, 58–62.

(17) Miller, P. R.; Skoog, S. A.; Edwards, T. L.; Lopez, D. M.; Wheeler, D. R.; Arango, D. C.; Xiao, X.; Brozik, S. M.; Wang, J.; Polsky, R.; et al. Multiplexed Microneedle-Based Biosensor Array for Characterization of Metabolic Acidosis. *Talanta* **2012**, 88, 739–742.

(18) Anastasova, S.; Crewther, B.; Bemnowicz, P.; Curto, V.; Ip, H. M.; Rosa, B.; Yang, G.-Z. A Wearable Multisensing Patch for Continuous Sweat Monitoring. *Biosens. Bioelectron.* **2017**, 93, 139–145.

(19) Parrilla, M.; Cuartero, M.; Padrell Sánchez, S.; Rajabi, M.; Roxhed, N.; Niklaus, F.; Crespo, G. A. Wearable All-Solid-State Potentiometric Microneedle Patch for Intradermal Potassium Detection. *Anal. Chem.* **2019**, 91, 1578–1586.

(20) Meruva, R. K.; Meyerhoff, M. E. Catheter-Type Sensor for Potentiometric Monitoring of Oxygen, PH and Carbon Dioxide. *Biosens. Bioelectron.* **1998**, 13, 201–212.

(21) Clark, L. C.; Duggan, C. A. Implanted Electroenzymatic Glucose Sensors. *Diabetes Care* **1982**, 5, 174–180.

(22) Frost, M. C.; Meyerhoff, M. E. Real-Time Monitoring of Critical Care Analytes in the Bloodstream with Chemical Sensors: Progress and Challenges. *Annu. Rev. Anal. Chem.* **2015**, 8, 171–192.

(23) Chung, H. J.; Sulkin, M. S.; Kim, J. S.; Goudeseune, C.; Chao, H. Y.; Song, J. W.; Yang, S. Y.; Hsu, Y. Y.; Ghaffari, R.; Efimov, I. R.; et al. Stretchable, Multiplexed PH Sensors with Demonstrations on Rabbit and Human Hearts Undergoing Ischemia. *Adv. Healthcare Mater.* **2014**, 3, 59–68.

(24) Li, G.; Li, Y.; Chen, G.; He, J.; Han, Y.; Wang, X.; Kaplan, D. L. Silk-Based Biomaterials in Biomedical Textiles and Fiber-Based Implants. *Adv. Healthcare Mater* **2015**, 4, 1134–1151.

(25) Jiang, X.; Wang, P.; Liang, R.; Qin, W. Improving the Biocompatibility of Polymeric Membrane Potentiometric Ion Sensors by Using a Mussel-Inspired Polydopamine Coating. *Anal. Chem.* **2019**, 6424–6429.

(26) Espadas-Torre, C.; Meyerhoff, M. E. Thrombogenic Properties of Untreated and Poly(Ethylene Oxide)-Modified Polymeric Matrices Useful for Preparing Intraarterial Ion-Selective Electrodes. *Anal. Chem.* **1995**, 67, 3108–3114.

(27) Wang, X. Overview on Biocompatibilities on Implantable Biomaterials. *Advances in Biomaterials Science and Biomedical Applications*; IntechOpen, 2013; Chapter 5, pp 111–155.

(28) Zdrachek, E.; Bakker, E. Potentiometric Sensing. *Anal. Chem.* **2019**, 91, 2–26.

(29) Papp, S.; Jágorszki, G.; Gyurcsányi, R. E. Ion-Selective Electrodes Based on Hydrophilic Ionophore-Modified Nanopores. *Angew. Chem., Int. Ed.* **2018**, 57, 4752–4755.

(30) Bobacka, J.; Ivaska, A.; Lewenstam, A. Potentiometric Ion Sensors. *Chem. Rev.* **2008**, 108, 329–351.

(31) Lewenstam, A. Routines and Challenges in Clinical Application of Electrochemical Ion-Sensors. *Electroanalysis* **2014**, 26, 1171–1181.

(32) Cuartero, M.; Crespo, G. A. All-Solid-State Potentiometric Sensors: A New Wave for in Situ Aquatic Research. *Curr. Opin. Electrochem.* **2018**, 10, 98–106.

(33) Zajac, M.; Lewenstam, A.; Stobiecka, M.; Dołowy, K. New ISE-Based Apparatus for Na<sup>+</sup>, K<sup>+</sup>, Cl<sup>−</sup>, PH and Transepithelial Potential Difference Real-Time Simultaneous Measurements of Ion Transport

across Epithelial Cells Monolayer—Advantages and Pitfalls. *Sensors* **2019**, 19, 1881–1894.

(34) Bandodkar, A. J.; Hung, V. W. S.; Jia, W.; Valdés-Ramírez, G.; Windmiller, J. R.; Martinez, A. G.; Ramírez, J.; Chan, G.; Kerman, K.; Wang, J. Tattoo-Based Potentiometric Ion-Selective Sensors for Epidermal PH Monitoring. *Analyst* **2013**, 138, 123–128.

(35) Moriuchi-Kawakami, T.; Tokunaga, Y.; Yamamoto, H.; Shibutani, Y. Ion-Selective Electrodes Based on L-Tryptophan and L-Tyrosine. *Talanta* **2012**, 94, 99–103.

(36) Pankratova, N.; Cuartero, M.; Cherubini, T.; Crespo, G. A.; Bakker, E. In-Line Acidification for Potentiometric Sensing of Nitrite in Natural Waters. *Anal. Chem.* **2017**, 89, 571–575.

(37) Bakker, E.; Bühlmann, P.; Pretsch, E. Polymer Membrane Ion-Selective Electrodes—What Are the Limits? *Electroanalysis* **1999**, 11, 915–933.

(38) Totu, E. E.; Spatarelu, C.; Maier, A. Ion-Selective Polymeric Membranes for Chemical Sensors. I. In *Recent Researches in Energy, Environment and Sustainable Development*; 2009, pp 161–165.

(39) Bakker, E.; Pretsch, E.; Bühlmann, P. Selectivity of Potentiometric Ion Sensors. *Anal. Chem.* **2000**, 72, 1127–1133.

(40) Wadey, B. L. Piezoelectric Polymers: Plasticizers. In *Encyclopedia of Polymer Science and Technology*; 2001, Vol 3, pp 498–525.

(41) Kim, J.; Campbell, A. S.; Esteban-Fernández de Ávila, B.; Wang, J. Wearable Biosensors for Healthcare Monitoring. *Nat. Biotechnol.* **2019**, 37, 389–406.

(42) Daniele, R. P.; Holian, S. K.; Nowell, P. C. A Potassium Ionophore (Nigericin) Inhibits Stimulation of Human Lymphocytes by Mitogens. *J. Exp. Med.* **1978**, 147, 571–581.

(43) Krotnę, M. A.; Bartoszewicz, M.; Świąćicka, I. Cereulide and Valinomycin, Two Important Natural Dodecadepsipeptides with Ionophoretic Activities. *Pol. J. Microbiol.* **2010**, 59, 3–10.

(44) Teplova, V.; Jääskeläinen, E.; Salkinoja-Salonen, M.; Saris, N. E. L.; Serlachius, M.; Li, F. Y.; Andersson, L. C. Differentiated Paju Cells Have Increased Resistance to Toxic Effects of Potassium Ionophores. *Acta Biochim. Pol.* **2004**, 51, 539–544.

(45) Qin, Y.; Peper, S.; Bakker, E. Plasticizer-Free Polymer Membrane Ion-Selective Electrodes Containing a Methacrylic Copolymer Matrix. *Electroanalysis* **2002**, 14, 1375–1381.

(46) Messori, M.; Toselli, M.; Pilati, F.; Fabbri, E.; Fabbri, P.; Pasquali, L.; Nannarone, S. Prevention of Plasticizer Leaching from PVC Medical Devices by Using Organic-Inorganic Hybrid Coatings. *Polymer* **2004**, 45, 805–813.

(47) Boisselier, E.; Astruc, D. Gold Nanoparticles in Nanomedicine: Preparations, Imaging, Diagnostics, Therapies and Toxicity. *Chem. Soc. Rev.* **2009**, 38, 1759–1782.

(48) Bian, D.; Deng, J.; Li, N.; Chu, X.; Liu, Y.; Li, W.; Cai, H.; Xiu, P.; Zhang, Y.; Guan, Z.; et al. In Vitro and in Vivo Studies on Biomedical Magnesium Low-Alloying with Elements Gadolinium and Zinc for Orthopedic Implant Applications. *ACS Appl. Mater. Interfaces* **2018**, 10, 4394–4408.

(49) Xu, M.; Zhu, J.; Wang, F.; Xiong, Y.; Wu, Y.; Wang, Q.; Weng, J.; Zhang, Z.; Chen, W.; Liu, S. Improved In Vitro and In Vivo Biocompatibility of Graphene Oxide through Surface Modification: Poly(Acrylic Acid)-Functionalization Is Superior to PEGylation. *ACS Nano* **2016**, 10, 3267–3281.

(50) Ray, T. R.; Choi, J.; Bandodkar, A. J.; Krishnan, S.; Gutruf, P.; Tian, L.; Ghaffari, R.; Rogers, J. A. Bio-Integrated Wearable Systems: A Comprehensive Review. *Chem. Rev.* **2019**, 119, 5461–5533.

(51) Jepps, O. G.; Dancik, Y.; Anissimov, Y. G.; Roberts, M. S. Modeling the Human Skin Barrier - Towards a Better Understanding of Dermal Absorption. *Adv. Drug Delivery Rev.* **2013**, 65, 152–168.

(52) Daniele, R. P.; Holian, S. K. A Potassium Ionophore (Valinomycin) Inhibits Lymphocyte Proliferation by Its Effects on the Cell Membrane. *Proc. Natl. Acad. Sci.* **1976**, 73, 3599–3602.

(53) Teplova, V. V.; Mikkola, R.; Tonshin, A. A.; Saris, N. E. L.; Salkinoja-Salonen, M. S. The Higher Toxicity of Cereulide Relative to Valinomycin Is Due to Its Higher Affinity for Potassium at



Physiological Plasma Concentration. *Toxicol. Appl. Pharmacol.* **2006**, *210*, 39–46.

(54) Hoornstra, D.; Andersson, M. A.; Mikkola, R.; Salkinoja-Salonen, M. S. A New Method for in Vitro Detection of Microbially Produced Mitochondrial Toxins. *Toxicol. In Vitro* **2003**, *17*, 745–751.

(55) Bandodkar, A. J.; Jeang, W. J.; Ghaffari, R.; Rogers, J. A. Wearable Sensors for Biochemical Sweat Analysis. *Annu. Rev. Anal. Chem.* **2019**, *12*, 1–22.

(56) Moody, G. J.; Saad, B. B.; Thomas, J. D. R. Studies on Bis(Crown Ether)-Based Ion-Selective Electrodes for the Potentiometric Determination of Sodium and Potassium in Serum. *Analyst* **1989**, *114*, 15–20.

(57) Yuan, D.; Anthi, A. H. C.; Ghahraman Afshar, M.; Pankratova, N.; Cuartero, M.; Crespo, G. A.; Bakker, E. All-Solid-State Potentiometric Sensors with a Multiwalled Carbon Nanotube Inner Transducing Layer for Anion Detection in Environmental Samples. *Anal. Chem.* **2015**, *87*, 8640–8645.

(58) Angello, J. C. Replicative Potential and the Duration of the Cell Cycle In Human Fibroblasts: Coordinate Stimulation by Epidermal Growth Factor. *Mech. Ageing Dev.* **1992**, *62*, 1–12.

(59) Abdian, N.; Ghasemi-Dehkordi, P.; Hashemzadeh-Chaleshtori, M.; Ganji-Arjenaki, M.; Doosti, A.; Amiri, B. Comparison of Human Dermal Fibroblasts (HDFs) Growth Rate in Culture Media Supplemented with or without Basic Fibroblast Growth Factor (BFGF). *Cell Tissue Banking* **2015**, *16*, 487–495.

(60) Guinovart, T.; Parrilla, M.; Crespo, G. A.; Rius, F. X.; Andrade, F. J. Potentiometric Sensors Using Cotton Yarns, Carbon Nanotubes and Polymeric Membranes. *Analyst* **2013**, *138*, S208–S215.

(61) Guinovart, T.; Bandodkar, A. J.; Windmiller, J. R.; Andrade, F. J.; Wang, J. A Potentiometric Tattoo Sensor for Monitoring Ammonium in Sweat. *Analyst* **2013**, *138*, 7031–7038.

(62) Bandodkar, A. J.; Jeeran, I.; You, J.-M.; Nuñez-Flores, R.; Wang, J. Highly Stretchable Fully-Printed CNT-Based Electrochemical Sensors and Biofuel Cells: Combining Intrinsic and Design-Induced Stretchability. *Nano Lett.* **2016**, *16*, 721–727.

(63) Akindoyo, J. O.; Beg, M. D. H.; Ghazali, S.; Islam, M. R.; Jeyaratnam, N.; Yuvaraj, A. R. Polyurethane Types, Synthesis and Applications-a Review. *RSC Adv.* **2016**, *6*, 114453–114482.

(64) Kim, K. M.; Kim, Y. W.; Choi, B. K.; Yoon, H. J.; Paeng, K.-J.; Nam, H. Physical and Potentiometric Properties of Polyurethane-Based Cation-Selective Membranes. *J. Appl. Polym. Sci.* **2001**, *80*, 618–625.

(65) Dinten, O.; Spichiger, U. E.; Chaniotakis, N.; Gehrig, P.; Rusterholz, B.; Morf, W. E.; Simon, W. Lifetime of Neutral-Carrier-Based Liquid Membranes in Aqueous Samples and Blood and the Lipophilicity of Membrane Components. *Anal. Chem.* **1991**, *63*, 596–603.

(66) Yang, G.; Anastasova, S.; Chen, C. M.; Gil, B.; Ip, H.; Kassanos, P.; Thompson, A. J. In *Implantable Sensors and Systems*; Yang, G.-Z., Ed.; Springer, 2018; pp 1–646.

(67) Bühlmann, P.; Pretsch, E.; Bakker, E. Carrier-Based Ion-Selective Electrodes and Bulk Optodes. 2. Ionophores for Potentiometric and Optical Sensors. *Chem. Rev.* **1998**, *98*, 1593–1688.

(68) Suzuki, K.; Siswanta, D.; Otsuka, T.; Amano, T.; Ikeda, T.; Hisamoto, H.; Yoshihara, R.; Ohba, S. Design and Synthesis of a More Highly Selective Ammonium Ionophore than Nonactin and Its Application as an Ion-Sensing Component for an Ion-Selective Electrode. *Anal. Chem.* **2000**, *72*, 2200–2205.

(69) Doebl, J. A. Effects of Neutral Ionophores on Membrane Electrical Characteristics of NG108-15 Cells. *Toxicol. Lett.* **2000**, *114*, 27–38.

(70) Cuartero, M.; Ortuño, J. A.; García, M. S.; Sánchez, G.; Mäs-Montoya, M.; Curiel, D. Benzodipyrrole Derivates as New Ionophores for Anion-Selective Electrodes: Improving Potentiometric Selectivity towards Divalent Anions. *Talanta* **2011**, *85*, 1876–1881.

(71) Lindner, E.; Cosofret, V. V.; Ufer, S.; Buck, R. P.; Kao, W. J.; Neuman, M. R.; Anderson, J. M. Ion-Selective Membranes with Low

Plasticizer Content: Electroanalytical Characterization and Biocompatibility Studies. *J. Biomed. Mater. Res.* **1994**, *28*, 591–601.

(72) Radomska, A.; Singhal, S.; Ye, H.; Lim, M.; Mantalaris, A.; Yue, X.; Drakakis, E. M.; Toumazou, C.; Cass, A. E. G. Biocompatible Ion Selective Electrode for Monitoring Metabolic Activity during the Growth and Cultivation of Human Cells. *Biosens. Bioelectron.* **2008**, *24*, 435–441.

(73) Cosofret, V. V.; Nahir, T. M.; Lindner, E.; Buck, R. P. New Neutral Carrier-Based H<sup>+</sup> Selective Membrane Electrodes. *J. Electroanal. Chem.* **1992**, *327*, 137–146.

(74) Jonah, T. M.; Mathivathanan, L.; Morozov, A. N.; Mebel, A. M.; Raptis, R. G.; Kavallieratos, K. Remarkably Selective NH<sup>4+</sup> Binding and Fluorescence Sensing by Tripodal Tris(Pyrazolyl) Receptors Derived from 1,3,5-Triethylbenzene: Structural and Theoretical Insights on the Role of Ion Pairing. *New J. Chem.* **2017**, *41*, 14835–14838.

(75) Späth, A.; Knig, B. Molecular Recognition of Organic Ammonium Ions in Solution Using Synthetic Receptors. *Beilstein J. Org. Chem.* **2010**, *6*, 1–111.

(76) Meier, P. C. Two-Parameter Debye-Hückel Approximation for the Evaluation of Mean Activity Coefficients of 109 Electrolytes. *Anal. Chim. Acta* **1982**, *136*, 363–368.

(77) Bakker, E.; Pretsch, E. Modern Potentiometry. *Angew. Chem., Int. Ed.* **2007**, *46*, 5660–5668.

(78) Bakker, E. Determination of Unbiased Selectivity Coefficients of Neutral Carrier-Based Cation-Selective Electrodes. *Anal. Chem.* **1997**, *69*, 1061–1069.

(79) Pankratova, N.; Cuartero, M.; Jowett, L. A.; Howe, E. N. W.; Gale, P. A.; Bakker, E.; Crespo, G. A. Fluorinated Tripodal Receptors for Potentiometric Chloride Detection in Biological Fluids. *Biosens. Bioelectron.* **2018**, *99*, 70–76.

(80) Bakker, E.; Pretsch, E.; Bühlmann, P. Selectivity of Potentiometric Ion Sensors. *Anal. Chem.* **2000**, *72*, 1127–1133.

(81) Kimura, K.; Maeda, T.; Tamura, H.; Shono, T. Potassium-Selective PVC Membrane Electrodes Based on Bis- and Poly(Crown Ether)S. *J. Electroanal. Chem. Interfacial Electrochem.* **1979**, *95*, 91–101.

(82) Tamura, H.; Kumami, K.; Kimura, K.; Shono, T. Simultaneous Determination of Sodium and Potassium in Human Urine or Serum Using Coated-Wire Ion-Selective Electrodes Based on Bis(Crown Ether)S. *Mikrochim. Acta* **1983**, *80*, 287–296.

(83) Bariya, M.; Nyein, H. Y. Y.; Javey, A. Wearable Sweat Sensors. *Nat. Electron.* **2018**, *1*, 160–171.

(84) Krebs, H. A. Chemical Composition of Blood Plasma and Serum. *Annu. Rev. Biochem.* **1950**, *19*, 409–430.

(85) Nakhoul, G. N.; Huang, H.; Arrigain, S.; Jolly, S. E.; Schold, J. D.; Nally, J. V.; Navaneethan, S. D. Serum Potassium, End-Stage Renal Disease and Mortality in Chronic Kidney Disease. *Am. J. Nephrol.* **2015**, *41*, 456–463.

(86) DuBose, T. D. Regulation of Potassium Homeostasis in CKD. *Adv. Chronic Kidney Dis.* **2017**, *24*, 305–314.

(87) He, J.; Mills, K. T.; Appel, L. J.; Yang, W.; Chen, J.; Lee, B. T.; Rosas, S. E.; Porter, A.; Makos, G.; Weir, M. R.; et al. Urinary Sodium and Potassium Excretion and CKD Progression. *J. Am. Soc. Nephrol.* **2016**, *27*, 1202–1212.